

ARTICLE

Received 4 Oct 2011 | Accepted 19 Jan 2012 | Published 6 Mar 2012

DOI: 10.1038/ncomms1692

# The tRNA methyltransferase NSun2 stabilizes p16<sup>INK4</sup> mRNA by methylating the 3'-untranslated region of p16

Xiaotian Zhang<sup>1,\*</sup>, Zhenyun Liu<sup>1,\*</sup>, Jie Yi<sup>1</sup>, Hao Tang<sup>1</sup>, Junyue Xing<sup>1</sup>, Minqwei Yu<sup>2</sup>, Tanjun Tong<sup>1</sup>, Yongfeng Shang<sup>1</sup>, Myriam Gorospe<sup>3</sup> & Wengong Wang<sup>1</sup>

The impact of methylation of the 3'-untranslated region (UTR) of a messenger RNA (mRNA) remains largely unknown. Here we show that NSun2, a transfer RNA methyltransferase, inhibits the turnover of p16<sup>INK4</sup> mRNA. Knockdown of NSun2 reduces p16 expression by shortening the half-life of the p16 mRNA, while overexpression of NSun2 stabilizes the p16 mRNA. *In vitro* methylation assays show that NSun2 methylates the p16 3'UTR at A988. Knockdown of NSun2 reduces the stability of the EGFP-p16 chimeric reporter transcripts bearing wild-type p16 3'UTR, but not p16 3'UTR with a mutant methylation site. Methylation by NSun2 prevents the association of p16 3'UTR with HuR, AUF1 and Ago2/RISC, and prevents the recruitment of EGFP-p16 3'UTR chimeric transcripts to processing bodies. In response to oxidative stress, NSun2 is essential for elevating p16 expression levels. We conclude that NSun2-mediated methylation of the p16 3'UTR is a novel mechanism to stabilize p16 mRNA.

<sup>1</sup> Research Center on Aging, Department of Biochemistry and Molecular Biology, Peking University Health Science Center, 38 Xueyuan Road, Beijing 100191, PR China. <sup>2</sup> The First Clinical College, Wuhan University, 9 Ziyang Road, Wuhan 430060, PR China. <sup>3</sup> Laboratory of Molecular Biology and Immunology, National Institute on Aging, National Institutes of Health, 251 Bayview Blvd., Baltimore, Maryland 21224, USA. \*These authors contributed equally to this work. Correspondence and requests for materials should be addressed to W.W. (email: wwg@bjmu.edu.cn).

**M**ethylation is an important post-transcriptional modification for almost all species of RNA. The methylation of transfer RNA (tRNA) and ribosomal RNA (rRNA) has been described as a regulatory modification for processes such as the faithful ribosomal decoding<sup>1</sup>, the stabilization of tRNA<sup>2</sup>, ribosome assembly<sup>3</sup>, ribosomal recycling, and the accuracy of translation initiation<sup>4–5</sup>. A variety of cellular and viral messenger RNAs (mRNAs) were also found to contain methylated constituents. For example, the methylation of the mRNA 5′-cap has been intensively studied<sup>6–7</sup>. In addition, a few studies have described the methylation of other regions of an individual mRNA, such as intron-specific region of the bPRL mRNA<sup>8</sup> and the 3′-untranslated region (UTR) of bovine prolactin<sup>9</sup>. Although small amounts of N5-methylcytosine have been identified, mRNA methylation events predominantly occur as N6-methyladenosine. Methylation at an intron influences the processing of bPRL mRNA precursor and the accumulation of mature mRNA in the cytoplasm<sup>8</sup>. However, whether methylation within the 3′UTR of an individual mRNA can impact upon such processes as mRNA maturation, translation or turnover has not been elucidated.

NSun2 (NOP2/Sun domain family, member 2; Myc-induced SUN domain-containing protein, Misu) is a nucleolar RNA methyltransferase mediating c-Myc-induced proliferation of the skin by recruiting the nucleolar and spindle-associated protein<sup>10</sup>. The nucleolar localization of NSun2/Misu is dependent on RNA polymerase III transcripts, suggesting that NSun2 may target methylation of rRNA or tRNA. Indeed, *in vitro* methylation assays have proven that tRNA is a typical substrate of NSun2<sup>11–12</sup>. The subcellular distribution of NSun2 may link its methyltransferase activity to the cell division cycle. During interphase, NSun2 is concentrated in the nucleolus and interacts with nucleolar proteins NPM1/nucleophosmin/B23 as well as nucleolin/C23, thereby suppressing the methyltransferase activity of NSun2<sup>10</sup>. The phosphorylation of NSun2 at Ser139 by Aurora-B suppresses the methyltransferase activity of NSun2 by enhancing this association<sup>12</sup>. In mitosis and the G2 phase, NSun2 is present in the perichromosome and cytoplasm<sup>11</sup>. Although the biological impact of this distribution is not known, the observation that NSun2 is expressed highly in cancer as well as in the S phase of the cell cycle<sup>11</sup> suggests that NSun2-mediated RNA methylation may act as an important post-transcriptional regulator of cancer and cell proliferation genes. However, the methylation of specific mRNAs by NSun2 and the downstream consequences have not been reported.

In recent years, post-transcriptional regulatory events, especially the regulation of mRNA turnover and translation by RNA-binding proteins and microRNAs, have gained much recognition<sup>13–14</sup>. This regulation occurs largely via the interaction of target mRNAs (predominantly at their 3′UTR) and these post-transcriptional regulatory factors. The sequence and the secondary structure of mRNAs are also important for the association of mRNA with the regulatory factors as well as for the fate of the mRNA (for example, translation, turnover, and so on). For example, the secondary structure of a target mRNA is a key determinant for the binding of HuR or AUF1 to the target mRNA; a stem-loop structure located at the 3′UTR of p16 mRNA is necessary for the destabilizing influence of RNA-binding proteins HuR, AUF1 and Ago2 upon the p16 mRNA<sup>15</sup>.

In the present study, we show that NSun2-mediated methylation of the p16 3′UTR reduces p16 mRNA decay. We have identified A988 within the p16 3′UTR as the methylation site of NSun2. The methylation of p16 3′UTR prevents the mobilization of p16 mRNA into processing bodies, linked to the stabilization of p16 mRNA. This regulatory pathway is responsible for elevating p16 expression under oxidative stress.

## Results

**NSun2 induces p16 expression by stabilizing the p16 mRNA.** The finding that NSun2 mediates Myc-induced cell proliferation<sup>11</sup>

prompted us to ask if NSun2 regulates the expression of genes related to cell cycle progression. We tested if knockdown or overexpression of NSun2 influenced the levels of cell proliferation proteins, including cyclin A, cyclin B1, PCNA and p16. By western blot analysis, transfection of HeLa cells with a vector expressing NSun2 shRNA reduced the levels of NSun2 by ~85%, while transfection of the cells with a vector expressing NSun2 increased the levels of NSun2 by ~8.2-fold (Fig. 1a). Knockdown of NSun2 in HeLa cells reduced p16 levels by ~74%, whereas overexpression of NSun2 increased p16 levels by ~3.9-fold. However, neither knockdown nor overexpression of NSun2 altered the levels of cyclin A, cyclin B1, PCNA or glyceraldehyde-3-phosphate dehydrogenase (GAPDH).

As NSun2 has been described as an RNA methyltransferase, we asked if NSun2 regulates p16 expression at the post-transcriptional level. To begin to answer this question, the levels of p16 pre-mRNA and mRNA in cells treated as described in Figure 1a were assessed by real-time quantitative PCR (RT-qPCR) analysis. As shown in Figure 1b, neither knockdown nor overexpression of NSun2 markedly altered p16 pre-mRNA levels. In contrast, knockdown of NSun2 reduced p16 mRNA by ~77%, and overexpression of NSun2 increased the mRNA levels of p16 by ~3.7-fold (Fig. 1c). These results suggest that NSun2 may regulate the half-life of p16 mRNA. To test this hypothesis, the cells described in Figure 1a were used to analyse p16 mRNA half-life. As shown in Figure 1, the half-life of p16 mRNA in NSun2-silenced cells was markedly shorter ( $3.34 \pm 0.13$  h) than that observed in control shRNA-expressed cells ( $4.16 \pm 0.15$  h;  $P = 0.002$ , Student's *t*-test) (Fig. 1d), while the half-life of p16 mRNA in NSun2-overexpressing cells was longer ( $4.72 \pm 0.12$  h) than that in control vector-transfected cells ( $3.53 \pm 0.17$  h;  $P = 0.001$ , Student's *t*-test) (Fig. 1e). As a negative control, neither knockdown nor overexpression of NSun2 altered the half-life of  $\beta$ -actin mRNA. These data suggest that NSun2 may act as a stabilizer of p16 mRNA.

## NSun2 binds p16 3′UTR and stabilizes EGFP-p16 reporter RNAs.

Previous studies demonstrated that p16 mRNA turnover was regulated by HuR and AUF1<sup>15–17</sup>. To test if NSun2 similarly interacted with p16 mRNA, biotinylated fragments of p16 mRNA (coding region (CR), FL (full-length 3′UTR of p16), as well as 3′UTR fragments A, B, C, Ba, Bb and Bc (Fig. 2a, schematic)) and whole-cell extracts of HeLa cells were prepared and used for pull-down analysis. The presence of NSun2 in the pull-down materials was analysed by western blotting. HuR and HDAC1 served as a positive and negative control, respectively. As shown in Figure 2b, fragments FL, B and Bc interacted with NSun2, but fragments CR, A, C, Ba and Bb did not. HuR interacted with fragments FL, A, B and Bb, in agreement with previous findings<sup>15–16</sup>, while HDAC1 did not interact with any of the fragments used. These results suggested that the NSun2-response element may be located within fragment Bc.

To further test if NSun2 was associated with the p16 3′UTR directly, the interaction of purified His-NSun2 with <sup>32</sup>P-labelled fragments CR and B as well as with the fluorescein-labelled fragment B was assessed by *in vitro* RNA-protein-binding assays (rEMSA). The binding of His-HuR to fragment B served as a positive control. Both His-NSun2 and His-HuR were capable of binding to fragment B (Fig. 2), but not to fragment CR (Fig. 2c); the K<sub>d</sub> of the NSun2-p16B interaction was  $2277 \pm 216$  (Fig. 2d). Therefore, NSun2 is able to interact directly, albeit weakly, with the p16 3′UTR.

Next, we tested if the association of NSun2 with the p16 3′UTR affected the turnover of p16 mRNA. Several EGFP-derived reporter vectors bearing partial p16 fragments (Fig. 3a, schematic) were constructed. HeLa cells stably transfected with the pTet-off plasmid were individually co-transfected with each of the EGFP-p16 vectors plus a vector expressing either NSun2 shRNA or control shRNA. After 48 h, total RNA was prepared at the times indicated and the half-lives of the encoded chimeric RNAs were evaluated<sup>15–16</sup>. As shown in Figure 3b, knockdown of NSun2 significantly shortened

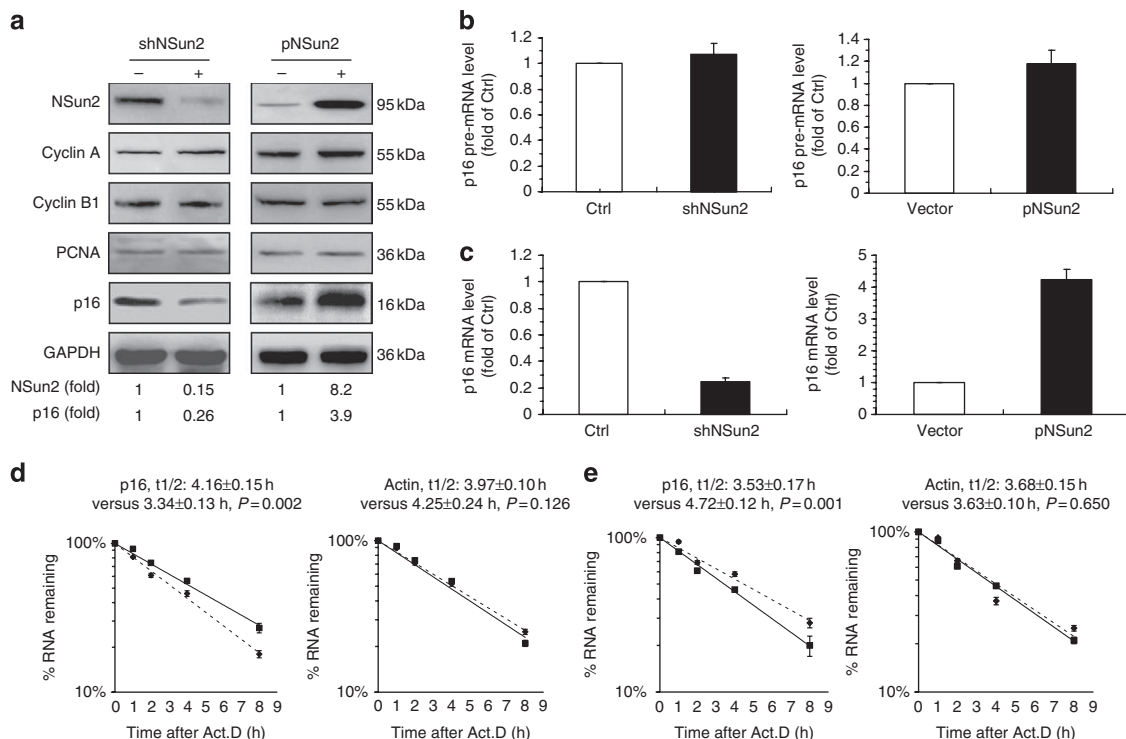


**Figure 1 | NSun2 regulates p16 expression by stabilizing p16 mRNA.** (a) At 48 h after transfection of HeLa cells with a vector expressing the NSun2 shRNA (shNSun2) or NSun2 (pNSun2), lysates were prepared to assess the levels of NSun2, cyclin A, cyclin B1, PCNA, p16 and loading control GAPDH by western blot analysis. (b) RNA isolated from cells described in a was subjected to RT-qPCR analysis (normalized to GAPDH mRNA) to assess the p16 pre-mRNA levels. (c) RNA isolated from cells described in a was subjected to RT-qPCR analysis to assess the p16 mRNA levels. (d) At 48 h after transfection with a vector expressing the NSun2 shRNA (shNSun2) or the control shRNA (Control), HeLa cells were exposed to actinomycin D (2 μg ml<sup>-1</sup>), whereupon the cellular RNA was isolated at times indicated. RT-qPCR against GAPDH was performed to assess the half-lives of p16 and β-actin mRNA (dotted curves, shNSun2; solid curves, control). (e) At 48 h after transfection with a vector expressing NSun2 (pNSun2) or the control vector (Vector), HeLa cells were exposed to actinomycin D (2 μg ml<sup>-1</sup>), whereupon the cellular RNA was isolated at times indicated. RT-qPCR was performed to assess the half-lives of p16 and β-actin mRNA (dotted curves, pNSun2; solid curves, vector). The RT-qPCR data are represented as means ± s.e.m. from three independent experiments. Western blots are representative of three or more experiments, and the signals were quantified by densitometry.

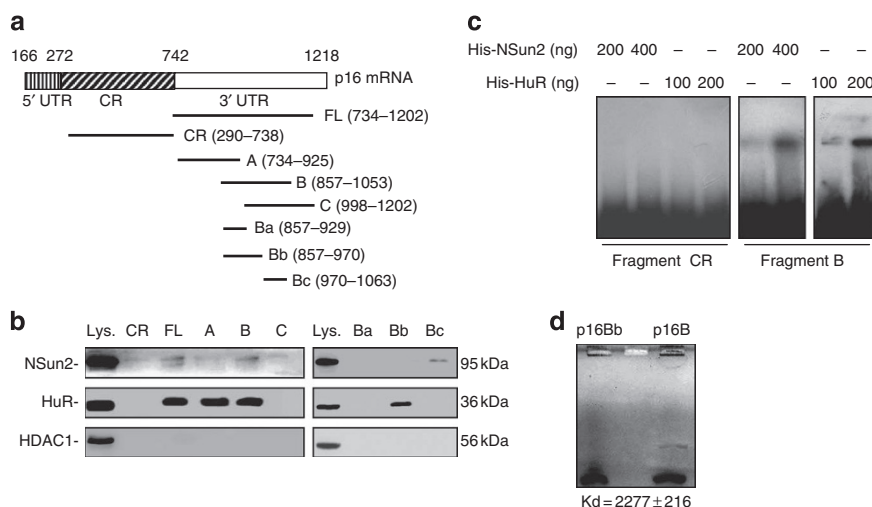


**Figure 2 | NSun2 interacts with the p16 3'UTR.** (a) Schematic representation of the p16 mRNA, depicting fragments used for biotin pull-down assays. (b) Biotin pull-down assays using the biotinylated fragments shown in a to detect bound cellular HuR and NSun2 by western blotting. A 10-μg aliquot of whole-cell lysate (Lys.) and binding to HDAC1 were included as controls. (c) *In vitro* protein-RNA-binding assays (EMSA) were performed using <sup>32</sup>P-labelled p16 fragments CR (coding region) and B as well as the indicated amounts of purified His-NSun2 (200–400 ng per reaction). Binding of His-HuR to the p16 3'UTR served as a positive control. (d) EMSA was performed using fluorescein-labelled p16 fragment B (0.003 nM) and purified His-NSun2 (0.003 nM). The dissociation constant (Kd) was estimated.

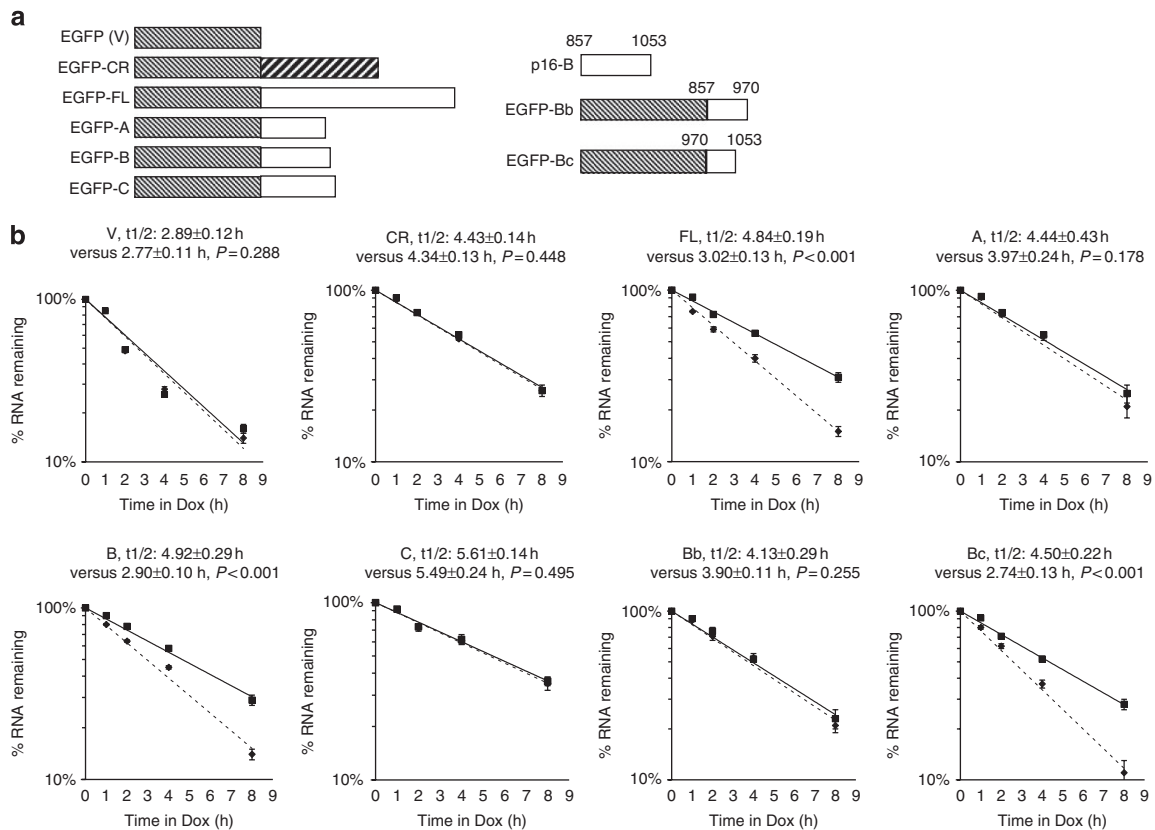


**Figure 3 | Influence of NSun2 on the stabilization of EGFP-p16 chimeric transcript.** (a) Schematic representation of the EGFP-p16 reporters studied. (b) HeLa cells stably transfected with pTet-Off plasmid were co-transfected with each of the EGFP-derived reporters bearing fragments of p16 mRNA (a, schematic), and a vector expressing NSun2 (shNSun2) or the control shRNA (control). After 48 h, the half-lives of the chimeric transcripts were assessed by RT-qPCR (dotted curves, shNSun2; solid curves, control).

the half-lives of the EGFP-FL ( $4.84 \pm 0.19$  h versus  $3.02 \pm 0.13$  h,  $P < 0.001$ , Student's *t*-test), EGFP-B ( $4.92 \pm 0.29$  h versus  $2.90 \pm 0.10$  h,  $P < 0.001$ , Student's *t*-test) and EGFP-Bc ( $4.50 \pm 0.22$  h versus  $2.74 \pm 0.13$  h,  $P < 0.001$ , Student's *t*-test). In contrast, the half-lives of EGFP, EGFP-CR, EGFP-A, EGFP-C, EGFP-Ba and EGFP-Bb mRNAs were not influenced. Therefore, the NSun2-response element is located in fragment Bc of the p16 3'UTR. As the response element of HuR, AUF1 and Ago2 is located at positions 929–960 (within the fragment B)<sup>15</sup>, our results indicate that the regulation of p16 mRNA turnover by NSun2 may be independent from the regulation by HuR, AUF1 and Ago2.

**NSun2 methylates the p16 3' UTR at A988.** NSun2 has been described as a tRNA methyltransferase. To test if NSun2 might be able to methylate p16 mRNA, *in vitro*-transcribed fragments of p16 mRNA (Fig. 2a) and purified His-NSun2 were used in *in vitro* methylation assays. <sup>3</sup>H incorporation to the p16 complementary DNA and to bacterial tRNA was included as negative and positive controls, respectively. As shown in Figure 4a, <sup>3</sup>H incorporation into FL p16 3'UTR was significantly higher than that observed from fragment UC (spanning the 5'UTR and p16-CR). Unlike the p16 3'UTR, <sup>3</sup>H incorporation into the 3'UTR of cyclin A, cyclin B1 and CDC25A was not significantly higher than that observed from p16 cDNA (Fig. 4b), suggesting that the methylation of p16 3'UTR by NSun2 is specific. Further study showed that NSun2 methylated fragments FL, B and Bc, but not fragments CR, A, C, Ba or Bb, indicating that the methylation site is located within fragment Bc (positions 970–1053) (Fig. 4c), which contained the NSun2-response element (Figs 2b,c and 3b). Fragment Bc contains an AAC (positions 987–989), but no GAC or CAA sequences. The AAC motif within

fragment B was then mutated as UAC (BΔ1), AUC (BΔ2) or AAU (BΔ3) by overlap PCR (Fig. 4d, schematic); C989 was not mutated to G because it would produce another consensus methylation motif (GAC). These mutated fragments were transcribed and subjected to *in vitro* methylation assays. As shown in Figure 4e, <sup>3</sup>H incorporation into fragments BΔ1, BΔ2 and BΔ3 was much lower than that seen with fragment B, indicating that the methylation site of p16 mRNA by NSun2 is located within the AAC motif. Notably, mutation of A987 and C989 exhibited similar effect as that of A988, in keeping earlier findings<sup>19</sup> that the context of the methylation site is also important for the methylation of RNA. We therefore conclude that the methylation site in p16 mRNA by NSun2 is located in A988 (Am<sup>6</sup>AC). To evaluate the efficiency of the methylation catalysed by NSun2, we performed titre assays and measured the initial velocity. <sup>3</sup>H incorporation into fragment B, but not into fragments CR, BΔ1, BΔ2 and BΔ3, increased when the amount of His-NSun2 increased (Fig. 4f). The estimated initial velocity was  $718 \pm 111$  (<sup>3</sup>H incorporation (CPM) min<sup>-1</sup>) for fragment B and  $831 \pm 130$  (<sup>3</sup>H incorporation (CPM) min<sup>-1</sup>) for tRNA methylation; the methylation of both tRNA and p16 fragment B was ~40% completed within 1 min (Supplementary Fig. S1a,b). The methylation efficiency of fragment B was estimated to be  $\geq 55.7\%$  (Supplementary Table S1). Therefore, the methylation of p16 mRNA catalysed by NSun2 is fast and efficient. In addition, a similar methylation motif (AAC) was conserved in the p16 3'UTR of Chimpanzee, but not in that of mouse or rat (Supplementary Fig. S1c), suggesting that the methylation of p16 3'UTR by NSun2 may occur only in primates.

**Methylation at A988 stabilizes the EGFP-p16 reporter RNAs.** To evaluate the influence of NSun2-mediated methylation on the

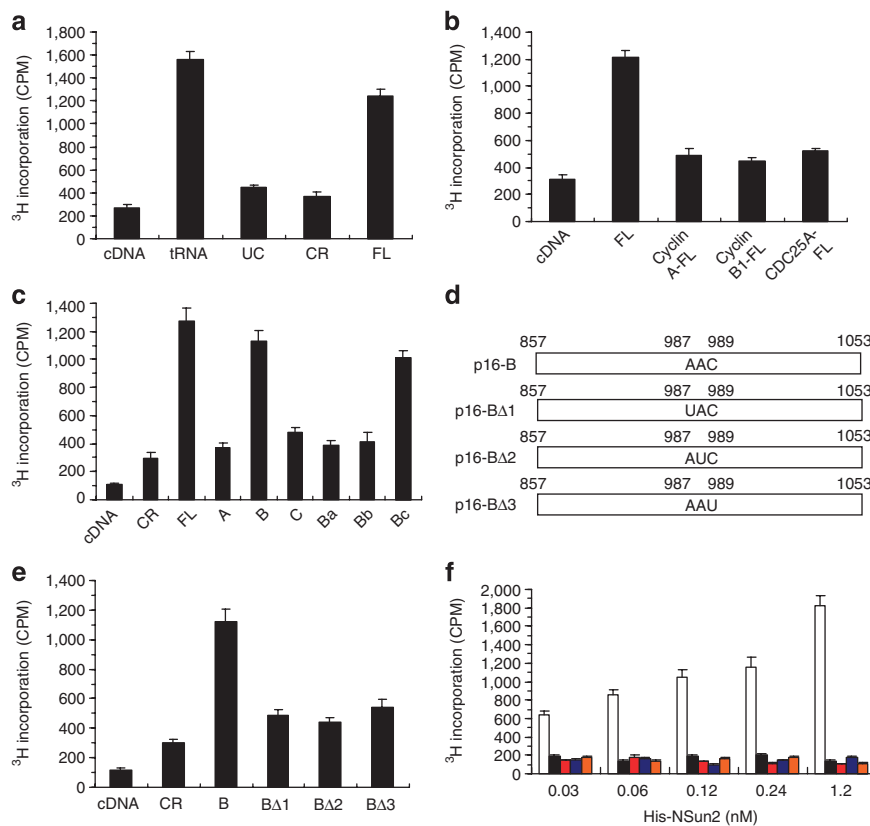


**Figure 4 | NSun2 methylates p16 mRNA at A988.** (a) Incorporation of  $^3\text{H}$ -labelled S-adenosyl-L-methionine (SAM) into p16 fragments UC, CR and 3'UTR. The incorporation of  $^3\text{H}$ -labelled SAM into p16 cDNA and tRNA bacteria served as negative and positive controls, respectively. (b) Incorporation of  $^3\text{H}$ -labelled SAM into the full-length (FL) 3'UTR of cyclin A, cyclin B1 and CDC 25A mRNAs. The p16 cDNA and FL 3'UTR served as negative and positive controls, respectively. (c) Incorporation of  $^3\text{H}$ -labelled SAM into different fragments of p16 mRNA. The p16 cDNA served as a negative control. (d) Schematic representation of p16-B mutants showing the positions of point mutation. (e) Incorporation of  $^3\text{H}$ -labelled SAM into p16-B and different mutants depicted in d. (f) Incorporation of  $^3\text{H}$ -labelled SAM into fragments B (white columns), CR (black columns), B $\Delta$ 1 (red columns), B $\Delta$ 2 (blue columns) and B $\Delta$ 3 (orange columns) by His-NSun2 at dose indicated. The *in vitro* methylation data represent the means  $\pm$  s.d. from three independent experiments.

half-life of p16 mRNA, B $\Delta$ 1, B $\Delta$ 2, B $\Delta$ 3 and B $\Delta$ 4 mutants depicted in Figure 5a were inserted into the pTRE-d2-EGFP vector (Fig. 5a, schematic). The B $\Delta$ 4 mutant (AAC to AUC) was derived from B1 fragment, a mutant fragment that was not a target of HuR, AUF1 or Ago2<sup>15</sup>. The effect of NSun2 knockdown on the half-lives of these reporter transcripts was assessed. As expected, knockdown of NSun2 shortened the half-life of EGFP-B mRNA ( $4.93 \pm 0.36$  h versus  $3.10 \pm 0.13$  h,  $P = 0.001$ , Student's *t*-test), but not those of EGFP-B $\Delta$ 1, EGFP-B $\Delta$ 2, EGFP-B $\Delta$ 3 and EGFP-B $\Delta$ 4 mRNAs (Fig. 5b). In addition, the half-life of EGFP-B1 mRNA, bearing the mutated HuR/AUF1-binding site, was also shortened by NSun2 silencing ( $4.49 \pm 0.12$  h versus  $2.77 \pm 0.11$  h,  $P < 0.001$ , Student's *t*-test). Therefore, methylation by NSun2 may act as a stabilizing modification of p16 mRNA and function independently of the HuR/AUF1-p16 regulatory process.

In previous studies, we reported that p16 mRNA was destabilized by AUF1, HuR and Ago2/RISC<sup>15</sup>. We further asked if NSun2-mediated methylation influenced the association of p16 mRNA with HuR, AUF1 and Ago2. To answer this question, HeLa cells were transfected with plasmids pGL3-B, pGL3-B $\Delta$ 2, pGL3-B1 or pGL3-CR (Fig. 6a, schematic). The association of fragments B, B $\Delta$ 2 and CR with HuR, AUF1 and Ago2, as well as the association of fragments B, B1, CR and B $\Delta$ 2 with NSun2, were assessed by RNP IP assays. The presence of Luc-CR chimeric transcript in the IP materials of HuR, AUF1, Ago2 or NSun2, and the presence of Luc-B, Luc-B $\Delta$ 2, Luc-B1 or Luc-CR chimeric transcripts in the IP materials of IgG

antibody were included as negative controls. As shown in Figure 6 by RT-qPCR from the IP materials, although the level of luciferase (Luc)-B $\Delta$ 2 chimeric transcript was  $\sim 30\%$  lower than that of pGL3-B transcript (input), the presence of Luc-B $\Delta$ 2 chimeric transcript in the IP materials of HuR, AUF1 and Ago2 was significantly higher than that of Luc-B (Fig. 6b). However, the presence of Luc-B1 and Luc-B $\Delta$ 2 chimeric RNAs in the NSun2 IP materials was comparable to that of Luc-B chimeric RNA (Fig. 6c,d). Further evidence was obtained from the biotin pull-down assays using *in vitro* methylated fragment B. As shown in Figure 6e, the presence of HuR, but not NSun2, in the pull-down material of methylated fragment B was reduced by  $\sim 61\%$  ( $P < 0.001$ , Student's *t*-test), compared with that of unmethylated fragment B. These results suggest that methylation by NSun2 antagonizes the binding of HuR to the p16 3'UTR; but neither the binding by HuR/AUF1 nor the methylation by NSun2 influenced the interaction of NSun2 with the p16 3'UTR. Furthermore, mutation of the methylation site increased the effect of HuR in inhibiting the activity of luciferase encoded by Luc-B $\Delta$ 2 RNA, while mutation of the HuR/AUF1-binding motif enhanced the effect of NSun2 in inducing the activity of Luc-B1-encoded luciferase (Fig. 6f,g). Moreover, although miR-24 was described as a repressor for p16 translation<sup>20</sup>, methylation by NSun2 had no influence on the interaction of p16 3'UTR with miR-24, miR-365 and miR125b (miR-365 and miR125b also target the p16 3'UTR, as determined using Target Scan) (Supplementary Fig. S2). Together, our results indicate that NSun2-mediated methylation of p16 3'UTR prevented

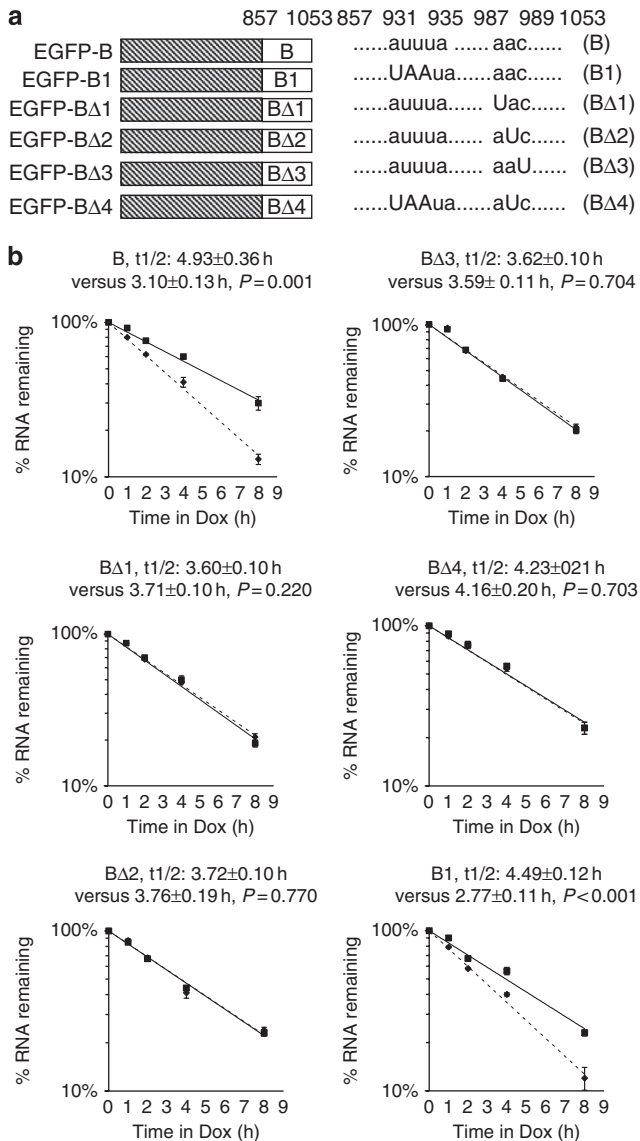


**Figure 5 | Methylation by NSun2 stabilizes the EGFP-p16 chimeric transcripts.** (a) Schematic representation of the EGFP-derived reporters bearing fragment B and different mutants of B fragment. The mutation site is indicated. (b) HeLa cells stably transfected with pTet-Off plasmid were co-transfected with EGFP-derived reporters bearing fragments B, BΔ1, BΔ2, BΔ3 and BΔ4 and a vector expressing NSun2 (dotted curves) or the control shRNA (solid curves). After 48 h, the half-lives of the chimeric transcripts were assessed by RT-qPCR.

the interaction of HuR/AUF1/Ago2/RISC with the p16 3'UTR, thereby antagonizing the effect of these RNA-binding proteins in destabilizing the p16 mRNA. Although binding by HuR/AUF1 did not influence the interaction of NSun2 with the p16 3'UTR, loss of HuR/AUF1 binding enhanced the effect of NSun2-mediated methylation in stabilizing p16 mRNA.

**Methylation at A988 reduces pMS2-p16 chimeric RNAs in PBs.** We previously described that the RISC component Ago2 destabilized p16 mRNA. As RISC has been implicated in the recruitment of mRNAs into PBs, we further asked if NSun2-mediated methylation of p16 3'UTR influences the colocalization of p16 mRNA with processing bodies (PBs). To address this question, the presence of the chimeric transcripts encoded by pMS2-B and pMS2-BΔ2 was evaluated. Co-transfection of pMS2, pMS2-B or pMS2-BΔ2 together with plasmid

pMS2-green fluorescent protein (GFP) (Fig. 7a, schematic) expressing the chimeric green fluorescent protein MS2-GFP with a nuclear localization signal<sup>21</sup> allowed us to track the subcellular localization of the chimeric MS2-B and MS2-BΔ2 RNAs (as the MS2-GFP-MS2-B and MS2-GFP-MS2-BΔ2 complex) as well as the control MS2 RNA (as the MS2-GFP-MS2 complex) by confocal microscopy. The MS2 system has been used successfully to track the subcellular localization of RNAs<sup>21-23</sup>. As shown in Figure 7b,c and previously reported<sup>21</sup>, the control MS2 RNA appeared to be exclusively nuclear in all of the transfected cells, owing to the presence of a nuclear localization signal in the MS2 fusion protein. By contrast, the GFP-MS2-B and MS2-BΔ2 RNAs were readily observed in the cytoplasm, colocalizing to some extent (but not exclusively) with RCK signals; the colocalization results in yellow signals in the merged images. The colocalization of MS2-GFP-MS2-B and RCK signals was reduced ~74% ( $P = 0.0006$ , Student's *t*-test) when NSun2 was overexpressed (Fig. 7b,d), while the colocalization of MS2-GFP-MS2-B and RCK signals was enhanced ~1.4-fold ( $P = 0.0074$ , Student's *t*-test) when NSun2 was silenced (Fig. 7c,e). Furthermore, in empty vector (pcDNA3.1) and control siRNA-transfected cells, the colocalization of MS2-GFP-MS2-BΔ2 and RCK signals was ~1.4-fold ( $P = 0.0139$ , Student's *t*-test) and ~1.5-fold ( $P = 0.0056$ , Student's *t*-test) higher than that of MS2-GFP-MS2-B and RCK signals, respectively. Moreover, neither overexpression nor silencing of NSun2 significantly altered the colocalization of MS2-GFP-MS2-BΔ2 and RCK ( $P = 0.9454$  for NSun2 overexpression,  $P = 0.1454$  for NSun2 knockdown, Student's *t*-test) (Fig. 7b-e). Together, these results suggest that NSun2 stabilizes p16 mRNA at least in part by protecting the transcript from transport into PBs.

**NSun2 stabilizes p16 mRNA under oxidative stress.** As the increased stability of p16 mRNA is responsible for the elevation of p16 under oxidative stress<sup>17</sup>, we further asked if NSun2-mediated methylation stabilizes the p16 mRNA in response to oxidative stress. Although exposure of HeLa cells to different doses of H<sub>2</sub>O<sub>2</sub> for 6 h increased the protein levels of p16 and NSun2, the maximum induction of NSun2 and p16 required at least 100 μM H<sub>2</sub>O<sub>2</sub> (Supplementary Fig. S3a). Exposure of the HeLa cells to a low dose (50 μM) of H<sub>2</sub>O<sub>2</sub> for 24 h, which increased the cells in G1 phase but did not trigger apoptosis (Supplementary Fig. S3b,c), significantly induced the protein levels of NSun2 and p16 (Fig. 8a). The induction of p16 by H<sub>2</sub>O<sub>2</sub> was mediated, at least in part, through stabilization of the p16 mRNA, as both the level and the half-life of p16 mRNA ( $2.78 \pm 0.13$  h versus  $4.28 \pm 0.12$  h,  $P < 0.001$ , Student's *t*-test) increased (Fig. 8a,b). To evaluate the contribution of NSun2-mediated methylation in the regulation of p16 under oxidative stress, the half-lives of EGFP-CR, EGFP-FL, EGFP-B, EGFP-B1, EGFP-BΔ2 and EGFP-BΔ4 chimeric transcripts were analysed. As shown in Figure 8c, under oxidative stress, the half-lives of transcripts EGFP-FL ( $2.57 \pm 0.10$  h versus  $4.00 \pm 0.13$  h,  $P < 0.001$ , Student's *t*-test), EGFP-B ( $3.22 \pm 0.14$  h versus  $4.55 \pm 0.18$  h,  $P = 0.001$ , Student's *t*-test), EGFP-BΔ2 ( $3.23 \pm 0.10$  h versus  $4.15 \pm 0.14$  h,  $P = 0.001$ , Student's *t*-test) and EGFP-B1 ( $3.08 \pm 0.12$  h versus  $4.78 \pm 0.10$  h,  $P < 0.001$ , Student's *t*-test) increased, but those of EGFP-CR or EGFP-BΔ4 mRNAs did not. Notably, EGFP-BΔ4 RNA, a mutant that was not a target of HuR, AUF1 or Ago2 and was not methylated by NSun2, was completely refractory to H<sub>2</sub>O<sub>2</sub> treatment. Furthermore, knock-down of NSun2 markedly diminished the effect of H<sub>2</sub>O<sub>2</sub> on inducing the expression of p16 (Supplementary Fig. S3d). In agreement to the observation from Figure 8c, the luciferase activity of pGL3-BΔ2 and pGL3-B1 reporters under oxidative stress was much lower than that encoded by pGL3-B, while the activity of pGL3-BΔ4 reporter (Supplementary Fig. S3e, schematic) was not altered by oxidative stress (Supplementary Fig. S3f). These results suggest that the stability of p16 mRNA under oxidative stress was regulated by both HuR/AUF1/Ago2-p16 and NSun2-p16 pathways, and the NSun2-

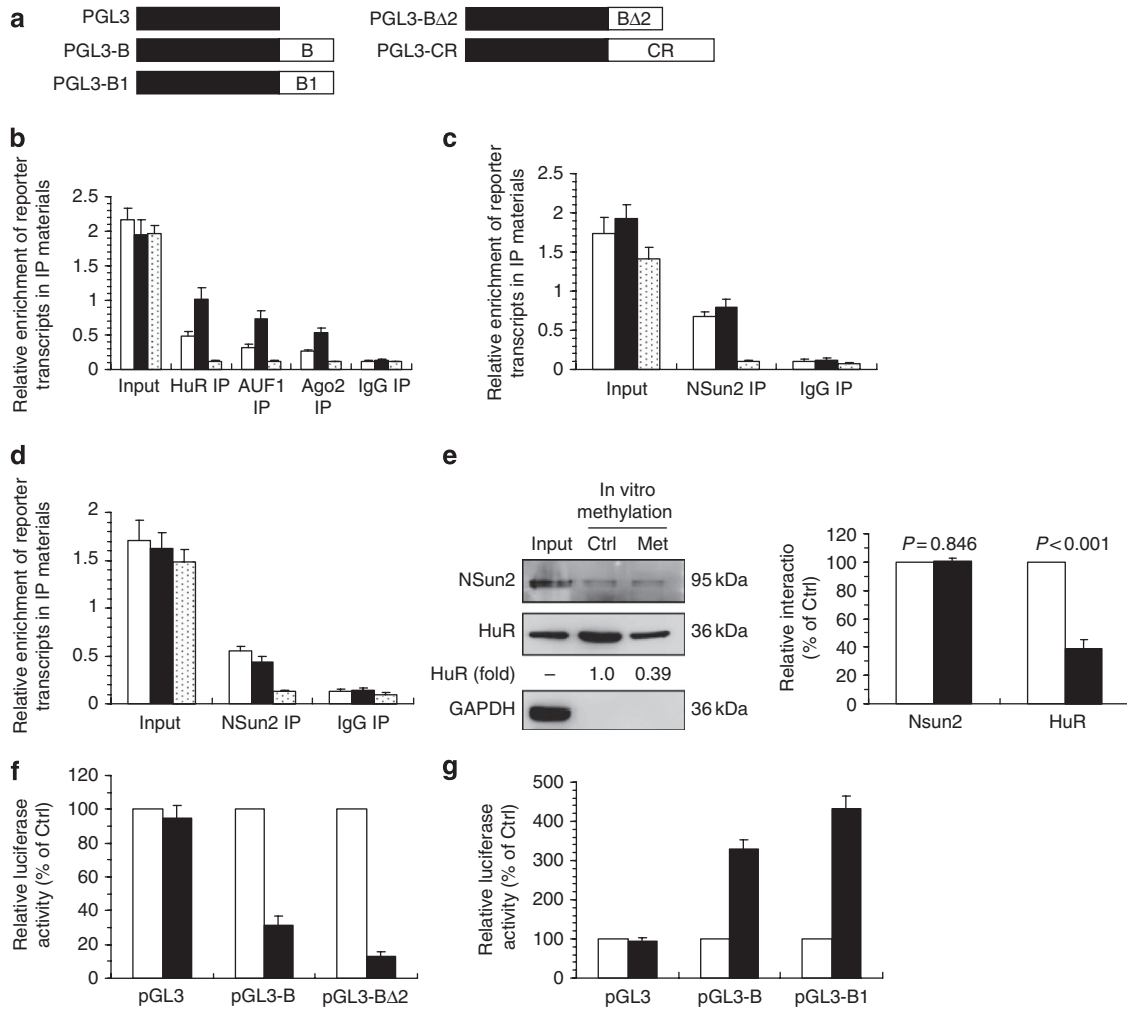


**Figure 6 | Methylation by NSun2 antagonizes the binding and functional influence of HuR and AUF1 upon the p16 3'UTR.** (a) Schematic representation depicts the pGL3-derived reporters. (b) At 24 h after transfection of HeLa cells with the plasmid pGL3-B, pGL3-BΔ2 or pGL3-CR, RNP IP assays were performed using HuR, AUF1, Ago2 or IgG antibody. The presence of chimeric transcripts Luc-B (white columns), Luc-BΔ2 (black columns) and Luc-CR (dotted columns) in the IP materials as well as their total levels (Input) were assessed by RT-qPCR. (c) At 24 h after transfection of HeLa cells with plasmid pGL3-B, pGL3-B1 or pGL3-CR, RNP IP assays were performed using NSun2 or IgG antibody. The presence of chimeric transcripts Luc-B (white columns), Luc-B1 (black columns) and Luc-CR (dotted columns) in the IP materials as well as their total levels (Input) were assessed by RT-qPCR. (d) At 24 h after transfection of HeLa cells with plasmid pGL3-B, pGL3-BΔ2 or pGL3-CR, RNP IP assays were performed using NSun2 or IgG antibody. The presence of Luc-B (white columns), Luc-BΔ2 (black columns) and Luc-CR (flecked columns) chimeric transcripts in the IP materials as well as their total levels (Input) was assessed by RT-qPCR. (e) Biotin pull-down assays were performed using *in vitro* methylated (nonisotopic) fragment B. The presence of NSun2 and HuR in the pull-down materials was assessed by western blotting. The means  $\pm$  s.d. from three assays (white columns, unmethylated; black columns, methylated) were used for the analysis of statistical significance by Student's *t*-test. (f) At 24 h after transfection with a vector expressing HuR (black columns) or an empty vector (white columns), HeLa cells were co-transfected with plasmids pGL3-B or pGL3-BΔ2 plus pRL-CMV reporter, and cultured for an additional 24 h. Firefly against Renilla luciferase activity was determined. (g) At 24 h after transfection with a vector expressing NSun2 (black columns) or an empty vector (white columns), HeLa cells were co-transfected with plasmids pGL3-B or pGL3-B1 plus pRL-CMV reporter, and cultured for an additional 24 h. Firefly against Renilla luciferase activity was determined. The RT-qPCR and luciferase assay data are represented as means  $\pm$  s.e.m. from three independent experiments.

p16 regulatory process was required for the utmost induction of p16 by oxidative stress.

**Discussion**

Altered mRNA turnover is an important post-transcriptional regulatory mechanism for a variety of mRNAs encoding cell cycle regulators such as p21<sup>CIP1</sup> and cyclins A, B1, D1 and E<sup>24–26</sup>, proliferation-associated genes such as *c-fos*<sup>27</sup>, as well as factors controlling tumour growth such as VEGF, COX-2,  $\beta$ -actin, tumour-necrosis factor- $\alpha$ , interleukin-6 and interleukin-8<sup>18,28–31</sup>. It is well known that RNA-binding proteins and microRNAs act as regulatory factors for mRNA turnover. In addition, the sequence and struc-

ture of mRNAs are also important determinants of mRNA stability. For example, a stem-loop structure of p16 3'UTR determines the effect of HuR and AUF1 to destabilize p16 mRNA<sup>15</sup>. As a typical tRNA methyltransferase, NSun2 was identified as a positive regulator of cell cycle progression<sup>11</sup>. However, ectopically increasing or decreasing NSun2 had no influence on the protein levels of cyclin A, cyclin B1 or PCNA (Fig. 1a). Instead, our findings indicate that methylation of p16 3'UTR by NSun2 may act as a stabilizing factor for p16 mRNA (Figs 1,3,5 and 8), which encodes a well-known inhibitor of cell proliferation. In our ongoing studies, we are screening for targets of NSun2 other than p16 mRNA by using cDNA/protein arrays and investigating whether NSun2-mediated

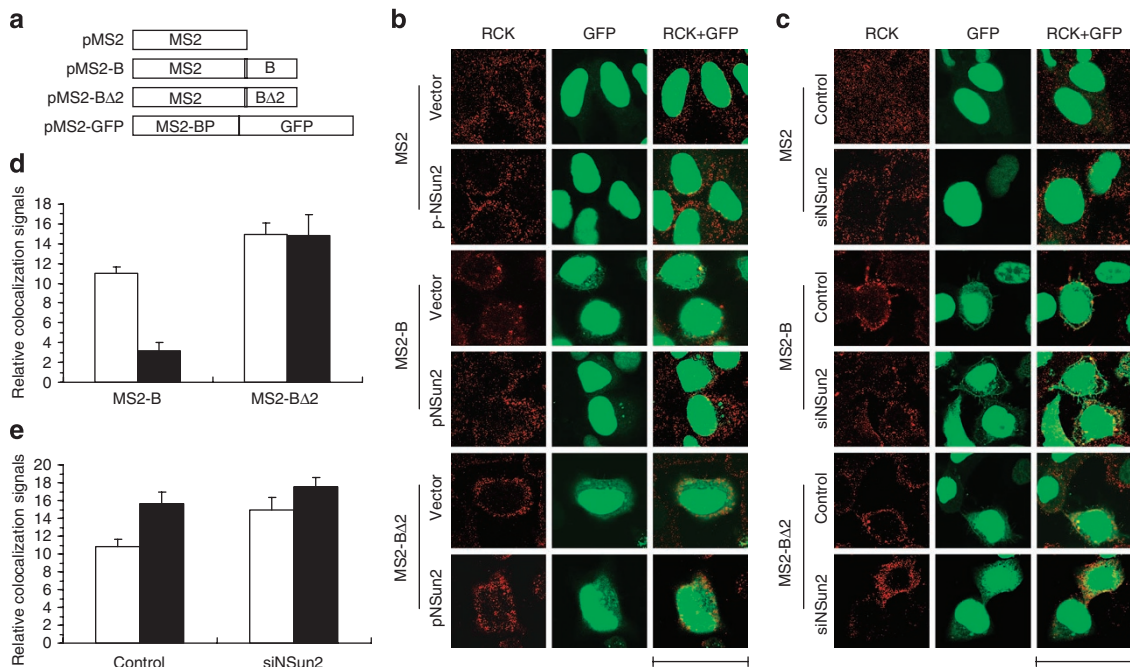


**Figure 7 | Methylation by NSun2 protects the recruitment of MS2-B chimeric transcripts to p-bodies.** (a) Schematic representation depicting the reporter vectors used for the p-body assays. (b) 24 h after co-transfection of HeLa cells with pSL-GFP-MS2 and either pSL-MS2, pSL-MS2-B or pSL-MS2-B $\Delta$ 2, cells were further transfected with vector expressing NSun2 (pNSun2) or the empty vector (Vector), and cultured for an additional 24 h. Using confocal microscopy, MS2, MS2-B and MS2-B $\Delta$ 2 RNAs were visualized using MS2-GFP (GFP, green fluorescence), and RCK signals (RCK, red immunofluorescence) were detected and colocalized (RCK + GFP, yellow). (c) 24 h after co-transfection of HeLa cells with pSL-GFP-MS2 and either pSL-MS2, pSL-MS2-B or pSL-MS2-B $\Delta$ 2, cells were further transfected with siRNA targeting NSun2 (siNSun2) or the control siRNA (Control), and cultured for an additional 24 h. The MS2, MS2-B and MS2-B $\Delta$ 2 RNAs were visualized using MS2-GFP, and RCK signals were detected and colocalized with the GFP signals. Where indicated, a scale bar indicated the size of the images ( $\sim$ 28  $\mu$ m). (d) The relative colocalization signals of GFP and RCK in (b) (percentage of (GFP + RCK) from total GFP signals in the cytoplasm) were calculated (white columns, Vector; black columns, pNSun2). (e) The relative colocalization signals of GFP and RCK in (c) (percentage of (white columns, Control siRNA; black columns, siNSun2)) were calculated. Data of the relative colocalization signals of GFP and RCK are represented as the means  $\pm$  s.e.m. from three independent experiments. The statistical significance of the relative colocalization of GFP and RCK was analysed by Student's *t*-test.

methylation functions as a broad post-transcriptional mechanism to control cell proliferation. The results of this work will enhance our understanding of NSun2 function during the process of cell proliferation.

Although methylation at all four nucleotides (A, U, C and G) of RNA has been reported<sup>32–33</sup>, methylation of an mRNA at other than the 5'-cap occurs predominantly as N6-methyladenosine (m<sup>6</sup>A), with a small amount of m<sup>5</sup>C identified in mRNA isolated from cultured hamster cells<sup>8</sup>. The Am<sup>6</sup>AC and Gm<sup>6</sup>AC motifs were described as the consensus sequences for adenosine methylation of mRNA catalysed by RNA methyltransferase<sup>8,34</sup>. In keeping with these earlier reports, the AAC motif locating at positions 987–989 in the p16 3'UTR has been identified by *in vitro* methylation assays as the methylation site by NSun2 (Fig. 4). This motif appears to be conserved only among primates (Supplementary Fig. S1c). *In vitro* protein–RNA-binding assays and biotin pull-down assays suggest that NSun2 may be an RNA-binding protein (Fig. 2b,c,d). It appears that the p16 3'UTR associates with NSun2 more weakly than with HuR (Fig. 2b,c), although it can efficiently methylate fragment B (Supplementary Fig. S1b and Table S1). In addition, methylation may occur at the p16 pre-mRNA stage or on mature (but still nuclear) p16 mRNA; it is unlikely that methylation occurs in the cytoplasm because no colocalization signals between NSun2 and GFP-MS2-B was observed in the cytoplasm (data not shown). Although the specific mechanisms by which NSun2 stabilizes p16 mRNA are not fully understood, our data suggest that NSun2-mediated p16 3'UTR methylation has two main consequences: it prevents the association

of HuR and AUF1 (but not the association of miR-24, miR-365 or miR125b) with the p16 mRNA (Fig. 6b and Supplementary Fig. S2c), and it prevents the recruitment of p16 mRNA into PBs (Fig. 7). The stabilization of p16 mRNA by NSun2 may not be caused by NSun2 binding to the p16 3'UTR, as mutation of the methylation site has no influence on the association of NSun2 with the p16 3'UTR (Fig. 6d,e).

In previous studies<sup>15–17</sup>, we showed that HuR- and AUF1-regulated p16 mRNA decay is an important mechanism for the elevation of p16 in both oxidative stress-induced cellular senescence and replicative senescence. Therefore, it was of interest to us to study whether NSun2-mediated p16 mRNA stabilization was involved in the elevation of p16 during cellular senescence. Unfortunately, the reduced level of NSun2 during replicative senescence suggests that NSun2 is unable to stabilize the p16 mRNA in replicative senescence (unpublished data). Under oxidative stress conditions, the increased stability of p16 mRNA could be achieved by repression through the complex HuR/AUF1/Ago2-p16 mRNA<sup>17</sup> and by the activation of NSun2-p16 regulatory process, as the plasmid pEGFP-B $\Delta$ 4/pGL3-B $\Delta$ 4, but not pEGFP-B1/pGL3-B1 or pEGFP- $\Delta$ 2/pGL3-B $\Delta$ 2, completely lost its responsiveness to oxidative stress (Fig. 8c and Supplementary Fig. S3f). In addition, loss of the NSun2-p16 process enhances the effect of HuR/AUF1 on regulating p16 expression under oxidative stress and vice versa (Fig. 6f,g). It is challenging to evaluate the contribution of NSun2-p16 or the HuR/AUF1-p16 regulatory process to the elevation of p16 under oxidative stress. However, the NSun2-p16 regulatory process is, at least in part, par-

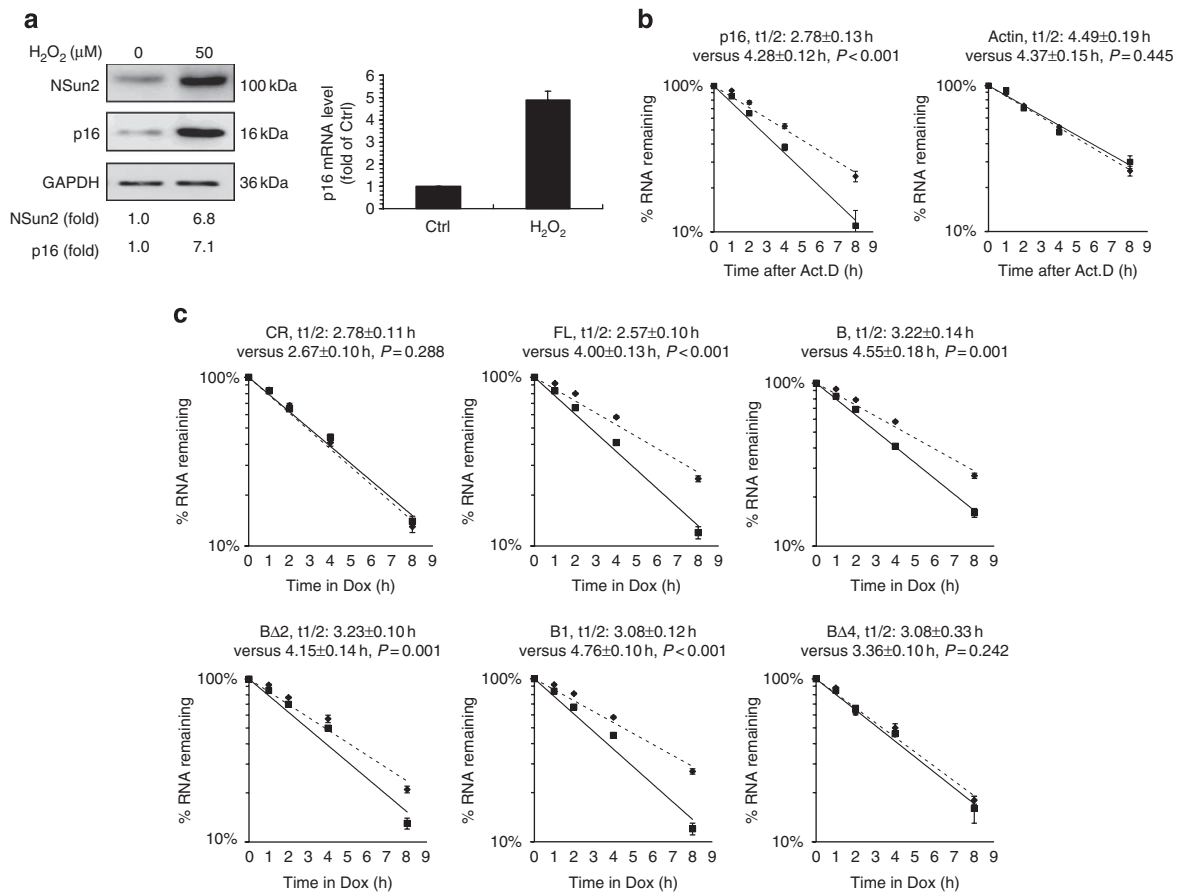


**Figure 8 | Induction of NSun2 and p16 in HeLa cells by H<sub>2</sub>O<sub>2</sub>.** (a) HeLa cells were exposed to H<sub>2</sub>O<sub>2</sub> (50 μM) for 24 h. The protein levels of NSun2, p16 and GAPDH were analysed by western blot analysis and the levels of p16 mRNA were analysed by RT-qPCR. (b) 24 h after exposure to H<sub>2</sub>O<sub>2</sub> (50 μM), HeLa cells were treated with actinomycin D (2 μg ml<sup>-1</sup>); at the times indicated, total RNA was isolated and subjected to RT-qPCR analysis. The half-lives of p16 mRNA and β-actin were calculated after normalization to GAPDH mRNA (solid curves, untreated; dotted curves, H<sub>2</sub>O<sub>2</sub> treated). (c) HeLa cells stably transfected with pTet-Off plasmid were co-transfected with each of the EGFP-derived reporters bearing fragments CR, FL, B, B1, BΔ2 and BΔ4. After 24 h, cells were treated with H<sub>2</sub>O<sub>2</sub> (50 μM) for 24 h and the half-lives of the chimeric transcripts assessed by RT-qPCR (solid curves, untreated; dotted curves, H<sub>2</sub>O<sub>2</sub> treated).

participating in elevating p16 under oxidative stress (Supplementary Fig. S3d). Therefore, the turnover of p16 mRNA (or other transcripts) could be regulated by multiple pathways and the relative contribution of each pathway might vary depending on the stimulus or the cell status.

Although methylation in the 3'UTR of bovine prolactin was reported two decades ago, the consequences of this regulation have not been described. The present study demonstrates that NSun2-mediated methylation of p16 3'UTR can stabilize the p16 mRNA and enhance p16 expression. This study sets the stage for future work to investigate the influence of 3'UTR methylation in the control of the turnover of other mRNAs.

## Methods

**Cell culture.** HeLa cells were cultured in Dulbecco's modified Eagle's medium (Invitrogen) supplemented with 10% foetal bovine serum and antibiotics, at 37 °C in 5% CO<sub>2</sub>.

**Transfection and treatment of cells.** Cells at 50% confluence were treated with 50 μM H<sub>2</sub>O<sub>2</sub> (Sigma) and collected for analysis 24 h later. All plasmid transfections were performed using Lipofectamine 2000 (Invitrogen). Unless otherwise indicated, cells were analysed 48 h after transfection.

**Antibodies and western blot analysis.** Whole-cell extracts were prepared in 20 mM HEPES (pH 7.4), 50 mM β-glycerophosphate, 1% Triton X-100, 10% glycerol, 2 mM EGTA, 1 mM dithiothreitol plus protease inhibitor cocktail. Western blot analysis was performed using 1 μg ml<sup>-1</sup> polyclonal anti-cyclin A (Abcam),

1 μg ml<sup>-1</sup> polyclonal anti-cyclin B1 (Abcam), 0.25 μg ml<sup>-1</sup> polyclonal anti-PCNA (Abcam), 0.5 μg ml<sup>-1</sup> polyclonal anti-NSun2 (Abcam), 0.2 μg ml<sup>-1</sup> monoclonal anti-GAPDH (Abcam), 0.2 μg ml<sup>-1</sup> monoclonal anti-HuR (Santa Cruz Biotechnologies), 0.2 μg ml<sup>-1</sup> monoclonal anti-p16 (Santa Cruz Biotechnologies) or 1 μg ml<sup>-1</sup> polyclonal anti-AUF1 (Santa Cruz Biotechnologies).

**RNA isolation and RT-qPCR.** Total cellular RNA was prepared using the RNeasy Mini Kit (Qiagen). The levels of p16 mRNA, GAPDH mRNA, and transcripts derived from pGL3 and pEGFP plasmids (chimeric Luc and EGFP transcripts, respectively) were detected using the following primer pairs: 5'-TGGAGGCG GGGCGCTGCCA-3' and 5'-TCGTGCACGGGTGGGTGAGA-3' for p16 mRNA, 5'-CGAGTCAACGGATTGGTGGTAT-3' and 5'-AGCCTTCTCCAT GGTGAAGAC-3' for GAPDH mRNA, 5'-TACAACACAGCCACAACG-3' and 5'-ATCCTGCTCCTCCACCTCC-3' for pEGFP-derived reporter transcripts (EGFP RNA), and 5'-GATTACCAGGGATTTCAGT-3' and 5'-GACACCTTAG GCAGACC-3' for pGL3-derived transcripts (Luc RNA). The primers for RT-qPCR analysis of miR-24, miR-365 and miR-125b were from Ribo Biology (Beijing, China).

**RNA-protein interaction assays and UV crosslink RNP IP assays.** cDNA was used as a template for PCR amplification of the different p16 mRNA fragments. All 5' primers contained the T7 promoter sequence (5'-(T7)CCAAGCTTCTAATACG ACTCACTATAGGGAGA-3'). Fragments CR, FL, A, B, C and B1 were described previously<sup>15</sup>. To prepare templates for the fragments UC (5'UTR + CDS), Ba, Bb and Bc, we used the following primer pairs:

5'-(T7)AGGAAGAAAAGAGGAGGGGC-3' and 5'-TCAATCGGGGAT GTCTGA-3' for UC, 5'-(T7)AGAAAATAGAGCTTTTAAAAATGCTCGT-3' and 5'-ACATTTACGGTGTAGTGGGGGAAGG-3' for Ba, 5'-(T7)AGAAAATAGAGCTT TAAAAATGCGCTG-3' and 5'-TTACATTTTATAAAGAATATATAAAAAATG-3' for Bb, and 5'-(T7)AAAAGAAAAACACCGCTTCTGCTTTTCAC-3' and 5'-ACCACATGAATGTGCCTTAG-3' for Bc. To prepare templates for the 3'UTR of

cyclin A, cyclin B1 and CDC-25A, we used these primer pairs: 5'-(T7)CAATGAAA GACTGCCTTTGTT-3' and 5'-TTTTTTTTTTTTTAAGGTAACA-3' for cyclin A 3'UTR, 5'-(T7)CTTGAACTTGAGTTGGAGT-3' and 5'-TTTTTTTTTTTTTGT ATTTGAG-3' for cyclin B1 3'UTR, and 5'-(T7)GGGGCTGCGCCAGTCTCG-3' and 5'-CTCAACTTGCTCAGTGCTTA-3' for CDC-25A 3'UTR. To generate p16 fragment B mutants BA1, BA2 and BA3, as well as the fragment FL mutant FLA, the anticipated NSun2 methylation motif (AAC, positions 987–989) was mutated as UAC (BA1), AUC (BA2, FLA) and AAU (BA3) by overlapping PCR. The BA4 was generated by mutating the AAC of fragment B1<sup>15</sup> as AUC by overlapping PCR.

For biotin pull-down assays, PCR-amplified DNA was used for *in vitro* transcription in the presence of biotin-UTP<sup>15</sup>. One microgram of purified biotinylated transcripts was incubated with 100 µg of whole-cell lysates for 30 min at room temperature. Complexes were isolated using paramagnetic streptavidin-conjugated Dynabeads (Dyna, Oslo, Norway), and the pull-down material was analysed by western blotting.

To perform RNA–protein interaction assays (eRMSA), p16 fragments B and CR were transcribed *in vitro* in the presence of <sup>32</sup>P-UTP<sup>18</sup>. The reaction mixtures (0.02 ml) contained 50 mM Tris (pH 7.0), 150 mM NaCl, 0.25 mg ml<sup>-1</sup> tRNA, 0.025 mg ml<sup>-1</sup> bovine serum albumin, 2.6 fmol of <sup>32</sup>P-labelled RNA and protein as indicated. Mixtures were incubated at 37 °C for 10 min, whereupon 5 µl of reaction mixture was loaded on a 0.8% agarose gel in TAE buffer (40 mM Tris acetate and 1 mM EDTA). After electrophoresis (40 V, 2.5 h), gels were dried and exposed to X-ray film.

To measure the dissociation constant of the NSun2-p16 3'UTR interaction, p16 fragment B was transcribed *in vitro* in the presence of fluorescein-12-UTP (Roche). The eRMSA assay was performed using 0.003 nM of His-NSun2 and 0.003 nM of fluorescein-labelled fragment B<sup>18</sup>. The reaction mixture was loaded immediately on a 0.8% agarose gel in TAE buffer (40 mM Tris acetate and 1 mM EDTA). The signals were visualized under 520-nm wavelength light and quantitated by densitometric analysis with the ImageMaster VDS software. The K<sub>d</sub> was estimated as F<sub>1</sub>×F<sub>2</sub>/C<sup>2</sup> (F<sub>1</sub>, unbound probe; F<sub>2</sub>, unbound protein; and C, complex).

For crosslinking of RNP IP complexes, cells were exposed to UVC (400 mJ cm<sup>-2</sup>) and whole-cell lysates prepared for immunoprecipitation<sup>15</sup> using monoclonal HuR or Ago2, or with polyclonal AUF1 and NSun2 antibodies. Briefly, lysates were precleared (30 min, 4 °C) by using 5 µg of IgG1 and 20 µl of Protein-A Sepharose beads that had been previously swollen in NT2 buffer (50 mM Tris, pH 7.4/150 mM NaCl/1 mM MgCl<sub>2</sub>/0.05% Nonidet P-40) supplemented with 5% BSA. Lysates (200 µg) were incubated (16 h, 4 °C) with 20 µl of Protein-A Sepharose beads in the presence of 3 µg of antibody for 3 h at room temperature. The IP materials were washed twice with stringent buffer (100 mM Tris–HCl, pH 7.4, 500 mM LiCl, 0.1% Triton X-100, 1 mM dithiothreitol, 2 µg ml<sup>-1</sup> leupeptin, 2 µg ml<sup>-1</sup> aprotinin and 1 mM phenylmethylsulphonyl fluoride) and twice with the IP buffer. The transcripts present in the RNP complexes were analysed by RT–qPCR.

**RNA interference.** To silence NSun2 transiently, cells were transfected with plasmid pSuper.retro-NSun2 or with siRNA targeting NSun2 (5'-GAGATCCTCTCTCTATGATC-3') using Lipofectamine-2000 or Oligofectamine (Invitrogen), respectively. To silence HuR or AUF1 transiently, vectors pSuper.retro-HuR or pSilencer-AUF1<sup>15</sup> were transfected into cells using Lipofectamine-2000. Cells were collected 24–48 h after transfection for further analysis.

**Constructs and mRNA half-life measurement.** For constructing pGL3- and pTRE-d2EGFP-derived reporter plasmids, the p16 fragments were amplified by PCR using the primers without the T7 promoter sequence and inserted into the pGL3- or pTRE-d2EGFP vector (Clontech).

To construct the pSL-MS2-GFP vector, the YFP in pSL-MS2-YFP<sup>20</sup> was mutated into GFP (Y<sub>203</sub>T<sub>203</sub>, [TACACC]) and subcloned into pcDNA3.0. For constructing the MS2-B, MS2-BA2, MS2-FL and MS2-FLA, the PCR-amplified fragments B, BA2, FL and FLA of p16 were inserted into the pMS2 vector (6×MS2 repeats). For constructing the flag-MS2-GFP vector, the PCR product of MS2-GFP was inserted between EcoRI and XbaI sites of flag-CMV 9.1 vector (Sigma).

For the construction of vectors expressing NSun2, the FL CR of NSun2 was amplified by PCR using primers 5'-CCGAATTCATGGGGCGGCGGTGCGG GGGT-3' and 5'-CCGCTCGAGTACCGGGGTGGATGGACC-3' and inserted between EcoRI and XhoI sites of pcDNA3.1+ vector (Clontech). To construct pET-28a(+)-NSun2, the FL CR of NSun2 was amplified using PCR primers 5'-CCGAATTCATGGGGCGGCGGTGCGGGGT-3' and 5'-CCGCTCGAGT CACCGGGGTGGATGGACC-3', and inserted into the EcoRI and XhoI sites of the pET-28a+ vector.

To prepare vectors expressing NSun2 shRNA or control shRNA, oligonucleotides corresponding to shRNA targeting NSun2 (5'-GAGATCCTCTCTCTAT GATC-3') or a control shRNA (AAGTGTAGTAGATCACCAGGC) were inserted between the Hind III and Bgl II sites in pSuper.retro (Oligoengine).

To measure the half-life of endogenous p16 mRNA, actinomycin D (2 µg ml<sup>-1</sup>) was added into the cell culture medium and total RNA was prepared and subjected to RT–qPCR analysis using p16-specific primers. To test the half-lives of the EGFP-p16 chimeric transcripts, HeLa cells stably transfected with the pTet-Off plasmid were further transfected with each of the pEGFP-p16 constructs. After 24 h, expression of the EGFP-p16 chimeric transcripts was shut off by addition of Doxycyclin

(Dox, 2 µg ml<sup>-1</sup>), whereupon total RNA was prepared at the times indicated and the transcript half-lives were evaluated by RT–qPCR using EGFP-specific primers. The half-lives of the reporter transcripts were represented as the means ± s.d. from three independent experiments. The statistical significance was analysed by Student's *t*-test.

**In vitro methylation assays.** For *in vitro* methyltransferase assay, His-tagged NSun2 was expressed in *E. coli* and purified using Ni-NTA Agarose (Qiagen) following the manufacturer's instructions. Reaction mixtures (50 µl) containing 1 µg of His-NSun2 (1 µg, ~0.24 nM), 0.02 µg (~0.007 nM) of *in vitro* transcribed fragments of mRNA and 1 µCi of <sup>3</sup>H-labelled S-adenosyl-L-methionine (Amersham Bioscience) in reaction buffer (5 mM Tris–HCl (pH 7.5), 5 mM EDTA, 10% glycerol, 1.5 mM dithiothreitol and 5 mM MgCl<sub>2</sub>)<sup>35</sup> supplemented with inhibitors (leupeptin (1 µg ml<sup>-1</sup>), aprotinin (1 µg ml<sup>-1</sup>), 0.5 mM phenylmethylsulphonyl fluoride and RNasin (5 U µl<sup>-1</sup>)) were incubated for 60 min at 37 °C. *E. coli* tRNA (0.013 nM (0.2 µg), Sigma) and unmethylated DNA (p16 fragment B DNA, 0.0035 nM (0.04 µg)) were used as positive and negative controls, respectively. Unincorporated <sup>3</sup>H S-adenosyl-L-methionine was removed by using Microspin G25 columns and incorporated radioactivity was measured by liquid scintillation counting. The nonisotopic methylated fragment B was prepared using cold SAM (Sigma) and biotin-labelled fragment B under same conditions.

**Immunofluorescence and confocal microscopy.** At 48 h after transfection, cells were fixed with 4% formaldehyde, permeabilized with 0.5% Triton X-100, blocked with 5% BSA and incubated with primary antibodies recognizing RCK (1 µg ml<sup>-1</sup>) (Santa Cruz Biotechnology). Alexa 405- or TRITC-conjugated secondary antibodies (0.8 µg ml<sup>-1</sup>) (Invitrogen) were used to detect primary antibody–antigen complexes with different colour combinations as needed. Images were visualized using FV1000-ASW Olympus Micro with FV1000-ASV 1.6 Viewer image processing software. The images were acquired with 10×100×2 and merged using maximum intensity. The relative colocalization signals of GFP and RCK (percentage of (GFP + RCK) from total GFP signals in the cytoplasm) were calculated. Statistical significance for the relative colocalization of GFP and RCK was analysed by Student's *t*-test.

## References

- Kimura, S. & Suzuki, T. Fine-tuning of the ribosomal decoding center by conserved methyl-modifications in the Escherichia coli 16S rRNA. *Nucleic Acids Res.* **38**, 1341–1352 (2010).
- Schaefer, M. *et al.* RNA methylation by Dnmt2 protects transfer RNAs against stress-induced cleavage. *Genes Dev.* **24**, 1590–1595 (2010).
- Meyer, B. *et al.* The Bowen-Conradi syndrome protein Nep1 (Emg1) has a dual role in eukaryotic ribosome biogenesis, as an essential assembly factor and in the methylation of ψ1191 in yeast 18S rRNA. *Nucleic Acids Res.* **39**, 1526–1537 (2011).
- Das, G. *et al.* Role of 16S ribosomal RNA methylations in translation initiation in Escherichia coli. *EMBO J.* **27**, 840–851 (2008).
- Seshadri, A., Dubey, B., Weber, M. H. & Varshney, U. Impact of rRNA methylations on ribosome recycling and fidelity of initiation in Escherichia coli. *Mol. Microbiol.* **72**, 795–808 (2009).
- Cowling, V. H. Regulation of mRNA cap methylation. *Biochem. J.* **425**, 295–302 (2009).
- Shatkin, A. J. & Manley, J. L. The ends of the affair: capping and polyadenylation. *Nat. Struct. Mol. Biol.* **7**, 838–842 (2000).
- Carroll, S. M., Narayan, P. & Rottman, F. M. N6-methyladenosine residues in an intron-specific region of prolactin pre-mRNA. *Mol. Cell. Biol.* **10**, 4456–4465 (1990).
- Narayan, P. & Rottman, F. M. An *in vitro* system for accurate methylation of internal adenosine residues in messenger RNA. *Science* **242**, 1159–1162 (1988).
- Hussain, S. *et al.* The nucleolar RNA methyltransferase Misu (NSun2) is required for mitotic spindle stability. *J. Cell. Biol.* **186**, 27–40 (2009).
- Frye, M. & Watt, F. M. The RNA methyltransferase Misu (NSun2) mediates Myc-induced proliferation and is upregulated in tumors. *Curr. Biol.* **16**, 971–981 (2006).
- Sakita-Suto, S. *et al.* Aurora-B regulates RNA methyltransferase NSUN2. *Mol. Cell. Biol.* **18**, 1107–1117 (2007).
- Moore, M. J. From birth to death: the complex lives of eukaryotic mRNAs. *Science* **309**, 1514–1518 (2005).
- Keene, J. D. RNA regulons: coordination of post-transcriptional events. *Nat. Rev. Genet.* **8**, 533–543 (2007).
- Chang, N. *et al.* HuR uses AUF1 as a cofactor to promote p16<sup>INK4</sup> mRNA decay. *Mol. Cell. Biol.* **30**, 3875–3886 (2010).
- Wang, W., Martindale, J. L., Yang, X., Chrest, J. F. & Gorospe, M. Increased stability of the p16 mRNA with replicative senescence. *EMBO Rep.* **6**, 158–164 (2005).
- Guo, G. *et al.* Hydrogen peroxide induces p16 (INK4) through an AUF1-dependent manner. *J. Cell. Biochem.* **109**, 1000–1005 (2010).
- Levy, N. S., Chung, S., Furneaux, H. & Levy, A. P. Hypoxic stabilization of vascular endothelial growth factor mRNA by the RNA-binding protein HuR. *J. Biol. Chem.* **273**, 6417–6423 (1998).

19. Narayan, P., Ludwiczak, R. L., Goodwin, G. C. & Rottman, F. M. Context effects on N6-adenosine methylation sites in prolactin mRNA. *Nucleic Acids Res.* **22**, 419–426 (1994).
20. Lal, A. *et al.* p16<sup>INK4a</sup> translation suppressed by miR-24. *PLoS One* **3**, e1864 (2008).
21. Lee, E. K. *et al.* hnRNP C promotes APP translation by competing with FMRP for APP mRNA recruitment to P bodies. *Nat. Struct. Mol. Biol.* **17**, 732–739 (2010).
22. Fusco, D. *et al.* Single mRNA molecules demonstrate probabilistic movement in living mammalian cells. *Curr. Biol.* **13**, 161–167 (2003).
23. Balagopal, V. & Parker, R. Polysomes, P bodies and stress granules: states and fates of eukaryotic mRNAs. *Curr. Opin. Cell Biol.* **21**, 403–408 (2009).
24. Wang, W., Yang, X., Cristofalo, V., Holbrook, N. & Gorospe, M. Loss of HuR is linked to reduced expression of proliferative genes during replicative senescence. *Mol. Cell. Biol.* **21**, 5889–5898 (2001).
25. Lal, A. *et al.* Concurrent versus individual binding of HuR and AUF1 to common labile target mRNAs. *EMBO J.* **23**, 3092–3102 (2004).
26. Guo, X. & Hartley, R. S. HuR contributes to cyclin E1 deregulation in MCF-7 breast cancer cells. *Cancer Res.* **66**, 948–956 (2006).
27. Atasoy, U., Watson, J., Patel, D. & Keene, J. D. ELAV protein HuA (HuR) can redistribute between nucleus and cytoplasm and is upregulated during serum stimulation and T cell activation. *J. Cell. Sci.* **111**, 3145–3156 (1998).
28. Sengupta, S. *et al.* The RNA-binding protein HuR regulates the expression of cyclooxygenase-2. *J. Biol. Chem.* **278**, 25227–25233 (2003).
29. Dean, J. L. *et al.* The 3′ untranslated region of tumor necrosis factor alpha mRNA is a target of the mRNA-stabilizing factor HuR. *Mol. Cell. Biol.* **21**, 721–730 (2001).
30. Dormoy-Raclet, V. *et al.* The RNA-binding protein HuR promotes cell migration and cell invasion by stabilizing the beta-actin mRNA in a U-rich-element-dependent manner. *Mol. Cell. Biol.* **27**, 5365–5380 (2007).
31. Nabors, L. B., Gillespie, G. Y., Harkins, L. & King, P. H. HuR, a RNA stability factor, is expressed in malignant brain tumors and binds to adenine- and uridine-rich elements within the 3′ untranslated regions of cytokine and angiogenic factor mRNAs. *Cancer Res.* **61**, 2154–2161 (2001).
32. Björk, G. R. *et al.* Transfer RNA modification. *Annu. Rev. Biochem.* **56**, 263–285 (1987).
33. Persson, B. C., Gustafsson, C., Berg, D. E. & Björk, G. R. The gene for a tRNA modifying enzyme, m5U54-methyltransferase, is essential for viability in *Escherichia coli*. *Proc. Natl Acad. Sci. USA* **89**, 3995–3998 (1992).
34. Kane, S. E. & Beemon, K. Precise localization of m6A in Rous sarcoma virus RNA reveals clustering of methylation sites: implications for RNA processing. *Mol. Cell. Biol.* **5**, 2298–2306 (1985).
35. Fuks, F., Burgers, W. A., Brehm, A., Hughes-Davies, L. & Kouzarides, T. DNA methyltransferase Dnmt1 associates with histone deacetylase activity. *Nat. Genet.* **24**, 88–91 (2000).

### Acknowledgements

This work was supported by Grant 2007CB507400 from the Major State Basic Research Development Program of China; Grants 81070247, 30921062 and 30973147 from the National Science Foundation of China; and Grant B07001 (111 project) from the Ministry of Education of People's Republic of China. M.G. was supported by the National Institute on Aging-IRP, National Institutes of Health.

### Author contributions

Y.S., T.T., M.G. and W.W. designed the study. X.Z., Z.L., J.Y., H.T., J.X. and M.Y. performed the experiments. M.G. and W.W. wrote the paper.

### Additional information

**Supplementary Information:** accompanies this paper at <http://www.nature.com/naturecommunications>

**Competing financial interests:** The authors declare no competing financial interests.

**Reprints and permission** information is available online at <http://npg.nature.com/reprintsandpermissions/>

**How to cite this article:** Zhang, X. *et al.* The tRNA methyltransferase NSun2 stabilizes p16<sup>INK4</sup> mRNA by methylating the 3′-untranslated region of p16. *Nat. Commun.* **3**:712 doi: 10.1038/ncomms1692 (2012).

# Corrigendum: The tRNA methyltransferase NSun2 stabilizes p16<sup>INK4</sup> mRNA by methylating the 3'-untranslated region of p16

Xiaotian Zhang, Zhenyun Liu, Jie Yi, Hao Tang, Junyue Xing, Minqwei Yu, Tanjun Tong, Yongfeng Shang, Myriam Gorospe & Wengong Wang

*Nature Communications* 3:712 doi: 10.1038/ncomms1692 (2012); Published 6 Mar 2012; Updated 25 Oct 2013

Concern was raised over the level of processing of the images in Fig. 2b in this Article. Because the original blots were no longer available, the experiment was repeated and the results presented in the new Fig. 9 below. As shown in this figure, fragments FL, B and Bc interacted with NSun2, but fragments CR (coding region), A, C, Ba and Bb did not. HuR interacted with fragments FL, A, B and Bb, whereas GAPDH did not interact with any of the fragments used. These additional data are consistent with Fig. 2b and thus support our original conclusions.

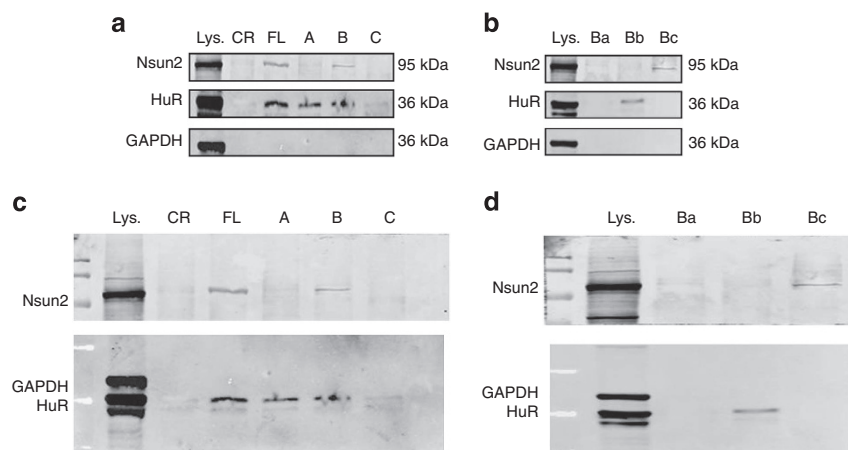


**Figure 9 | NSun2 associates with the 3'UTR of p16 mRNA.** (a) Biotin pull-down assays using p16 mRNA fragments CR, FL, as well as 3'UTR fragments A, B and C (Fig. 2a, schematic), to detect bound cellular NSun2 and HuR by western blotting. Controls included a 10  $\mu\text{g}$  aliquot of whole-cell lysate (Lys.) and immunoblotting for GAPDH. (b) Biotin pull-down assays were used to assess the association of NSun2 and HuR with p16 3'UTR fragments Ba, Bb and Bc (Fig. 2a, schematic), as described in a. (c,d) Full blots for panel a (c) and panel b (d). Western blot analysis was performed using 0.5  $\mu\text{g ml}^{-1}$  polyclonal anti-NSun2 antibody (Abcam), 0.2  $\mu\text{g ml}^{-1}$  monoclonal anti-HuR antibody (Santa Cruz Biotechnology) and 0.2  $\mu\text{g ml}^{-1}$  monoclonal anti-GAPDH antibody (CWBIO, Beijing).